Moroccan Journal of Chemistry
ISSN: 2351-812X
http://revues.imist.ma/?journal=morjchem&page=login
Kessraoui & al. / Mor. J. Chem. 5 N°4 (2017) 659-676

Non linear modelisation of dyes removal from aqueous solution by using sorption onto *Luffa cylindrica* fibers

A. Kesraoui[(a)*], M. Seffen[(a)], F. Brouers[(b)]

[(a)] *Laboratory of Energy and Materials (LABEM). High School of Sciences and Technology of Hammam Sousse, BP 4011Hammam Sousse (Sousse University-Tunisia). FP4BATIW project;*

[(b)] *Institute of Physics, B5 Sart Tilman, 4000, University of Liège, 4000 Liège, Belgium.*

Abstract

The biosorption of indigo carmine (IC) and methylene blue (MB) using a lingo-cellulosic fiber: *Luffa cylindrical* was carried out in this study. It was shown in this work, that biosorption capacity of dyes increase with increase of initial dyes concentrations and mass of biomass and to decrease with the raise of salt and temperature. Optimal parameters of the biosorption of dyes onto Luffa cylindrica were obtained after 150 min and pH 10 for MB and 525 min and pH 2 for IC. The experimental equilibrium data were studied employing the isotherms of Langmuir, Freundlich, Jovanovic, Temkin, Redlich–Peterson, Toth, Sips, and Brouers–Sotolongo. The experimental data fitted very well with the Bouers-Sotolongo isotherm for MB and the Toth isotherm for IC. Concerning IC, the value of maximum biosorption capacity (Q_m = 6.876 mg/g) was close to the experimental value (Q_m = 6.874 mg/g), and the correlation coefficient (R^2) was 0.996. While for MB, the value of maximum biosorption capacity (Q_m = 13.849 mg/g) was close to the experimental value (Q_m = 13.900 mg/g), and the correlation coefficient (R^2) was 0.992. In order to study the biosorption kinetics, four kinetics models such as pseudo-first order, pseudo-second order, Elovich and Brouers-Sotolongo were studied. The Brouers-Sotolongo (2,α) fractal model appears to be the best model to fit the experimental data.

* *Corresponding author:*
aida.kesraoui@gmail.com

Received 21 Dec 2016, Revised 23 July 2017, Accepted 19 Sept 2017

Keywords: Lignocellulosic materials; *Luffa cylindrica*; Biosorption; methylene blue; indigo carmin; Brouers-Sotolongo; Kinetics; Isotherms.

1. Introduction

Dyes are widely employed in textile, paper, plastic, food, and cosmetic industries [1]. Many dyes and their decompositions products contribute to water toxicity and constitute a danger for the environment, human and animals [2]. Indeed, dyes are with difficulty biodegradable and are not eliminated from wastewater by conventional wastewater treatment processes [3] because of their complex structure and synthetic origins [4]. Methylene blue (MB) is cationic dyes [5]. It is used in dye, paint production and wool dyeing [6] and has a recalcitrant character. The indigo carmine is an anionic dye [4]. It is largely employed for dyeing and printing protein and cellulose fibers [7]. The indigo Carmine is classified as very toxic dyes [8], its contact with the human body can provoke irritations of skin and eye, permanent damage with the cornea and the conjunctive one, gastro-intestinal irritation with nausea, vomiting and diarrhoea [9]. Different methods and their combinations are employed to remove dye from wastewater, like the ultrafiltration [10], electrodialysis [11], the adsorption on activated carbon [12] and biological treatment [13]. In fact the physicochemical treatments consume a large amount of oxidant [14] and sometimes lead to the formation of undesirable intermediate products [14]. Seen the low biodegradation of dyes, a biological treatment process is inefficient for eliminate dyes from wastewater [15]. Currently, adsorption methods are very interesting processes using natural materials that are frequently little or poor recovered [16, 17]. This method presents an advantage compared to the other processes because of its sludge free clean operation and totally eliminated dyes, even from the diluted solution [18]. Among these natural materials, we can cite mention macroalgae [19], Lansium domesticum [20], Calligonum polygonoides [21] and Mytilus edulis shells [9]. Luffa cylindrica is part of the Cucurbitaceae family [22]. His fibers may be employed by industry for packaging, insulation, or filling materials [23]. Luffa cylindrica fiber has a fibrous vascular system that may allow elimination of water pollutants [24]. Furthermore, several environmentally conscious consumers appreciate that Luffa cylindrica fibers are biodegradable, natural and renewable resources [25]. The objectives of this work were to investigate the chemical composition and characterization of *Luffa cylindrica*, determine optimum experimental conditions of biosorption of methylene blue and indigo carmine onto Lignocellulosic materials; *Luffa cylindrica* fibers and study the kinetics and isotherms mechanism. The biosorption kinetic modeling was studied by Lagregren, pseudo-second order, Elovich and Brouers Sotolongo models. On the other hand, the experimental equilibrium data were analyzed using the isotherms of Langmuir, Freundlich, Jovanovic,Temkin, Redlich–Peterson, Toth, Sips, and Brouers–Sotolongo.

2. Materials and methods

2.1. Biomass and dye solution preparation

The *Luffa cylindrica* fibers are used in this study as adsorbent. This biomass was bought at the local market of Sousse. First, the fibers were cut finely, washed several times with distilled water to suppress all impurities, and then dried in an oven at 70 °C for 48 h at a constant weight. Indigo carmine (Table 1) was used as a model anionic dye. Indigo carmine (or indigotin) is a blue dye (number E132) natural extract of the indigo plant. It belongs of the family of indigoids. The methylene blue (Table 1) was discovered by Caro in 1878. It is a basic cationic dye, heterocyclic aromatic chemical compound. The MB and IC were selected in this work as models of dyes due to their known strong adsorption onto solids. Stock solutions were prepared by dissolving 0.1 g of dye in a 1 L of distilled water. In order to obtain the needed concentrations, a stock solution was diluted with distilled water.

Table 1. Characteristics of IC and MB

Chemical name	Methylene blue	Indigo carmine
Chemical formula	$C_{16}H_{18}N_3SCl.$	$C_{16}H_8N_2Na_2O_8S_2$
Chemical structure	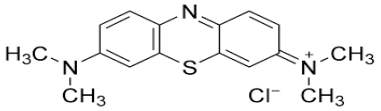	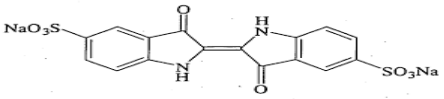
Molar mass (g mol^{-1})	319.85	466.36
λ_{max} (nm)	663	608
pKa	3.8	12.6

2.2. Sorption tests and analytical methods

To determine the chemical composition of *Luffa cylindrica*, a series of extractions were realized to isolate different substances contained in the material (fats and waxes, pectin, lignin, hemicellulose and lignin). The extraction protocol is described in the literature [[26]]. The milled fibers (10 g dry material) is extracted with 400 mL at 80% ethanol in a flask under stirring at 80 ° C by reflux for 20 min to remove fats and waxes. The degreased material is then extracted with water at 100 ° C (200 mL, 1 h), then with an aqueous solution of ammonium oxalate (1% by mass) heated by reflux at 85°C (300 mL, 2 h) to eliminate pectins. After, Lignins are extracted by two extractions in a mixture (400 mL) of sodium chlorite and glacial acetic acid (80 °C, 1 h) with stirring. Lignin is completly degraded by this treatment. Hemicelluloses are solubilized by a solution of potassium hydroxide (24% by mass) at 25 ° C (400 mL, 24 h) followed by a solution of sodium hydroxide (4.3% by mass) at 25 ° C (400 mL, 24 h) with stirring. Boehm's method was used to study the acidic functional groups [[27]] using basic solutions of different base strengths ($NaHCO_3$, Na_2CO_3, NaOH, C_2H_5ONa). A volume of 30 mL of these solutions was added to 0.5 g of *Luffa Cylindrica* fibers for 48 h. The excess of base was then determined by back titration using NaOH (0.05 mol L^{-1}) and HCl (0.025 mol L^{-1}). The point of zero charge (pH_{pzc}) was determined using the batch equilibrium method which proposed by Milongic et al. [[28]].

The biosorption experiments were realized by adding 0.6 g dried *Luffa cylindrica* fibers in 75 mL of dye solution (i.e. a solid/liquide ratio of 8 g/L) with the desired concentration (10-100 mg/L), pH (2-10) and temperature (293-343 K). All the experiences were carried out at 20 °C, with the exception of the experience performed to study the influence of temperature on biosorption. Temperature was controlled by a thermo-regulated water bath, model Memmert BME1420 operating at 105 oscillations × min^{-1}. All experiments were conducted in triplicate and the negative controls (without biomass) were simultaneously performed to verify that the biosorption capacity was due solely to biomass and did not involve the walls of the reactor. After biosorption, the residual dyes concentrations were determined by spectrophotometry double faisceaux analysis (FT-IR) (Camspec M550) at λ_{max} of 663 and 608 nm for MB and IC respectively. In order to analyze the functional groups in the *Luffa cylindrica*, the Fourier transform infrared spectrometry (PerkinElmer Spectrum two) has been used. The transmission spectrum was acquired with 4 cm^{-1} resolution and the spectrum was corrected for a KBr background. In order to characterize the surface morphology and fundamental physical properties of the *Luffa cylindrica*, the Scanning Electron Microscopy (SEM) has been used. SEM was carried out by using a JEOL JSM 5400 Scanning Microscope after coating them with gold using a JEOL JFC-1199E ion sputtering device.

2.3. Kinetics studies

In order to perform kinetic studies, 3 mL of the dye solution were taken periodically and then analyzed to determine the dye concentration. The evaluation of dye removal was performed by determination of the biosorption capacity at

equilibrium time (Qe) or by biosorption removal efficiency; have been determined respectively according to the following equations:

$$Q = \frac{(C_0 - C_i) \times V}{M} \quad (1)$$

$$\%dye\ removal = \frac{(C_0 - C_i) \times 100}{C_0} \quad (2)$$

where C_0 is the initial dye concentration (mg/L), C_i is the residual dye concentration at any time (mg/L), V is the volume of solution (L) , M is the mass of the biosorbent (g), At equilibrium, C_i is equal to Ce and Q is equal to Qe.

The model of pseudo-first-order, the pseudo-second-order, Elovich and Brouers-sotolongo equation [29,30,31] were used to fit the experimental data of the dye biosorption before reaching equilibrium. The differential equation is generally expressed as follow (Eq.3):

$$\frac{dQ}{dt} = k_1(Q_e - Q) \quad (3)$$

The linearized form of the pseudo-first-order model is determined by expression 4:

$$\log(Q_e - Q) = \log(Q_e) - \frac{k_1 \cdot t}{2{,}303} \quad (4)$$

where t is the time (min) ;k_1 is the equilibrium rate constant of pseudo-first-order sorption (min^{-1}). Unlike the pseudo-first-order model, the pseudo-second-order model is applicable to a larger interval of time [32]. The pseudo-second-order model is based on the sorption capacity of the solid phase is described by the equation 5:

$$\frac{dQ}{dt} = k_2(Q_e - Q)^2 \quad (5)$$

By integration Equation 5, the expression is simplified and linearized to obtaion equation 6:

$$\frac{t}{Q} = \frac{1}{k_2 \cdot Q_e^2} + \frac{t}{Q_e} \quad (6)$$

where k_2 is the equilibrium rate constant of pseudo-second-order adsorption (g/mg min). Also, the Elovich model is based on the adsorption capacity [30]. It is generally expressed by equation 7:

$$\frac{dQ}{dt} = B_E exp(-A_E Q) \quad (7)$$

The equation 7 can be simplified after integration by equation 8:

$$Q = \frac{1}{A_E} Ln(B_E \times A_E) + \frac{1}{A_E} Ln(t) \quad (8)$$

Where B_E is the initial adsorption rate (mg/g.min); A_E is the desorption constant (g/mg) The Brouers–Sotolongo model generalized fractal kinetic equation was developed to provide a universal function for the kinetics of complex systems characterized by stretched exponential and/or power law behaviours. This kinetic model unifies and generalizes previous theoretical attempts to describe what has been called “fractal kinetic”. More details on the mathematical development of this model and its application to biophysics and biotechnology are described in Brouers and Sotolongo article [33,34]. The pseudo BSf (n,α) sorption kinetics equation is given by expression (9):

$$Q(t) = Q_e \left[1 - \left(1 + (n-1)\left(\frac{t}{\tau}\right)^{\alpha}\right)^{\frac{-1}{n-1}}\right] \quad (9)$$

Where α as the fractal time exponent, n is an effective non-integer reaction order, τ a characteristic time, Qe the sorbed quantity at saturation , Q(t) the sorbed quantity at time t.

Eq.9 is a solution of a fractal differential equation [31,34] where a fractal time index a arising from the assumed fractal diffusion and sorption kinetics due to the geometric and energetic heterogeneity of the sorbent.has been empirically introduced :

$$-\frac{dq_{(t)}}{dt^a} = K_{a,n} q_{(t)}^n \quad (10)$$

The half sorption time (the time at wich half of the sorbed material has been adsorbed is a function of the three quantities a, n and τ (Eq. 10):

$$\tau_{50\%} = \tau\left(\frac{2^{(n-1)} - 1}{n-1}\right)^{1/\alpha} \quad (11)$$

The BSf(n,a) kinetics equation has many advantage [34]. It is a well-known statistical function (the BurrXII cumulative function) [35]. It can be obtained from the Boltzmann-Shannon entropy maximization with constraints on the average of the integrated Burr XII hazard function [36]. According to this principle, it is the less bias mathematical form knowing the three quantities Q_e, *n*, *a* and $\tau_{50\%}$. It allows tocalculate $\tau_{50\%}$, the time necessary to sorbed half of the maximum sorbed quantity, and the effective rate as a function of time as well as its maximum value. There exist in the literature more sophisticated theories to investigate the complex interplay between fractal diffusion and fractal reaction. They cannot, however provide simple formulas to treat macroscopic data such as the ones obtained here. They give asymptotic behaviors in agreement with those of the macroscopic formula BSf(n,a). By giving particular values to the coefficients, the *BS(n,a)* equation leads to four approximate cases, the first two are: the pseudo first and pseudo second order kinetics models. These two models have been commonly used in the literature. The two others are: the Weibull fractal first order (ffo) or the Avrami- Hill fractal second order kinetics (fso) models which are gaining more popularity. The four cases are:

a) If $n=1, \alpha=1$, one gets from eq (10) :

$$-\frac{dQt)}{dt} = K_1 q(t) \quad (12)$$

the solution of this equation is in our case:

$$Q(t) = Q_m(1-\exp(t/\tau)) \quad (13)$$

which is a first-order kinetics with $\tau = K_1^{-1}$ and $\tau_{50\%} = \tau(log2)$ and is equivalent to eq.(3)

b) If $, n=2,$ $\alpha=1$, eq (12) will become:

$$-\frac{dQ(t)}{dt} = K_2 Q(t)^2 \quad (14)$$

The solution of eq(14) is:

$$Q(t) = Q_m\left(\frac{t/\tau}{1+t/\tau}\right) \quad (15)$$

Where $\tau = (K_2 Q_m)^{-1} K_2$ is the second order constant and $\tau_{50\%} = \tau.$

Eq(10) can be transformed to the very popular pseudo second order kinetics

$$\frac{1}{Q_m - Q(t)} = K_2 t + \frac{1}{Q_m} \text{ or } \frac{t}{q(t)} = \frac{1}{K_2 Q_m^2} + \frac{1}{Q_m} \quad (16)$$

equivalent to eq. (6)

c) If $n=1, a \neq 1$, one gets the Weibull kinetics or Avrami kinetics BS(n,a) (in the theory of crystallization).

$$Q(t) = Q_m(1-\exp(t/\tau)^a) \quad (17)$$

With $\tau_{50\%} = \tau(log2)^{1/a}$

d) If $n=2, a \neq 1$, we have the Hill kinetics or fractal second order kinetics *BS(2,a)* or Hill kinetics.

$$Q(t) = Q_m \frac{(t/\tau)^a}{(1+(t/\tau)^a)} \quad (18)$$

Where $\tau = (K_{2,a} Q_m)^{-1/a}$ and $\tau_{50\%} = \tau$

2.4. Evaluation of equilibrium isotherms

The isotherms of two parameters (Langmuir [37], Freundlich [38], Jovanovic [39] and Temkin [40]) and three parameters (Sips [41], Redlich–Peterson [41], Brouers–Sotolongo [33] and Toth [41]) were investigated. Table 2 shows the equations and parameters of such isotherms.

Qm =maximum adsorption capacity; K_L = Langmuir constant; K_F , n_F = Freundlich constants; K_J = Jovanovic constant; b_T , k_T = Temkin constants; R = universal gas constant; T = absolute solution temperature in Kelvin; A_{RP}, B_{RP}, g = Redlich–Peterson constants; b_{To}, n_{To} = Toth constants; K_S, m_S = Sips constants; Kw, α, ، = Brouers–Sotolongo constants.

Table 2. Mathematical equations of the used isotherm models.

Isotherm model	Equation
Brouers-Sotolongo	$Qe = Q_{max}\ (1-\exp(-k_w * Ce^{\alpha}))$ (21) [33]
Redlich–Peterson	$Q_e = \frac{A_{RP} C_e}{1+B_{RP} C_e^{g}}$ (22) [41]
Sips	$Q_e = \frac{Q_m (k_S C_e)^{m_S}}{1+(k_S C_e)^{m_S}}$ (23) [41]
Toth	$Q_e = Q_m C_e \left(b_{T_0} + C_e^{n_{T_0}}\right)^{-\frac{1}{n_{T_0}}}$ (24) [41]
Langmuir	$Qe = Qmax * kL * \frac{Ce}{1+KL*Ce}$ (25) [37]
Freundlich	$Qe = k_F * Ce^{1/n}$ (26) [38]
Temkin	$Qe = \frac{RT}{bt} \ln (kt*Ce)$ (27) [40]
Jovanovic	$Q_e = Q_m \left(1 - exp\left(k_j C_e\right)\right)$ (28) [39]

2.5. Evaluation of thermodynamic parameters

Thermodynamic parameters such as free energy change (ΔG°), enthalpy change (ΔH°), and entropy change (ΔS°) for the biosorption of MB and IC on *Luffa cylindrica* was calculated according the following equations [14]:

$$\Delta G^{\circ} = -RT\ ln\ K_C = \Delta H^{\circ} - T\Delta S^{\circ} \quad (19)$$

where R is the gas constant (8.314 J mol^{-1} K^{-1}), T is the absolute temperature (K) and Kc is the apparent equilibrium constant Kd, defined according the equation 20 [15]:

$$K_C = \frac{C_{ad,eq}}{C_{r,eq}} \quad (20)$$

where Cad,eq and Cr,eq being the concentration of adsorbed dye at equilibrium and remaining concentration dye at equilibrium respectively (mg/L).

2.6. Error estimation

Nonlinear chi-square ($\chi 2$) test is a statistical tool needful for the best fit of a biosorption method, got by judging the sum squares differences between the experimental and the calculated data, with each squared difference is divided by its corresponding value (calculated from the models). A low value shows its similarities while a higher value indicates the variation of the experimental data [42]. The nonlinear chi-square test was calculated by equation 29 [42]:

$$\chi^2 = \sum_{i=1}^{n} \frac{\left(Q_{e,calc} - Q_{e,exp}\right)^2}{Q_{e,exp}} \quad (29)$$

3. Results and discussion

3.1. Chemical composition of Luffa cylindrica

The results obtained by the Boehm titration method were presented in table 3. The results show that the majority of acidic functional groups are carboxylic followed by lactonic and then phenolic. Moreover, the quantity of basic and the total quantity of acidic groups are approximately equal. These results suggest that *Luffa cylindrica* fibers had amphoteric character. The pH_{pzc} of *Luffa cylindrica* was proved to be 7.85. This result shows that the *Luffa cylindrica* surface has a positive charge at pH values less than the pH_{pzc} and therefore should be able to absorb anions and has negative charge at pH values higher than the pH_{pzc} and thus should be able to absorb cations. The dissociation of surface oxygen complexes of acid groups (carboxylic, lactones and phenol) gives a negative charge of the *Luffa cylindrica* surface [27]. Thus, the surface acid sites are of Bronsted type [27]. Concerning the positive charge, it may be due to existence of oxygen complexes of basic character such as pyrones or chromenes [27]. Also, it can be due to the presence of electron-rich regions within the graphene layers playing the role as Lewis basic centers, which accept

protons from the aqueous solution [27]. The *Luffa cylindrica* fibers are composed by: 7.10 % wax and grease, 4.70% pectine, 11.20% lignin, 23.00% hemicellulose and 54.00% cellulose. When compared with data for Vine shoots [43] or Eucalyptus globulus [44] or date palm rachis [45], it appears that cellulose and hemicellulose contents are relatively close. The pictine and lignin content of *Luffa cylindrica* is relatively low. The comparison with vine stems [46] confirms that the amounts of extractives fractions in the *Luffa cylindrica* are high. With regard to structural components, the *Luffa cylindrica* fibers are characterized by relatively low lignin content and high amounts of cellulose.

Table 3. pH_{PZC} value and Boehm titration results of extracted cellulose.

pH_{PZC}	Acidic groups (mmol/g)				Basic groups (mmol/g)
	Carboxylic	Phenolic	Lactonic	Total	
7.85	1.12	0.01	0.05	1.18	1.09

In order to determine the main functions present in *Luffa cylindrica* fibers, IR analysis was carried out in the region from 4000 to 400 cm^{-1}. The FT-IR spectrum of *Luffa cylindrica* fibers (Fig.1) shows the presence of a strong band at 3400 cm^{-1} which is assigned to –OH groups [14]. The peak presents at 2920 cm^{-1} correspond to –CH stretching vibration, corresponding to the aliphatic fragments of the cellulose [14]. The peak at 1737 cm^{-1} is attributed to carbonyl C=O which exists in carboxylic groups [47]. In addition, the band at 1429 cm^{-1} can be assigned to phenolic –OH and C–O stretching. The C–O stretching of ester, ether or phenol group were observed at 1254 and 1034 cm^{-1} [48].

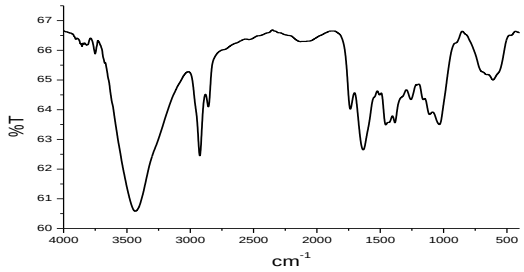

Figure 1. FT-IRspectrum of *Luffa cylindrica* fibers

Scanning electron microscopy (SEM) has been used for characterizing the surface morphology of *Luffa cylindrica*. Figure 2 shows that the *Luffa cylindrica* surface is composed by multicellular fibers. In addition, Figure 2.b shows the existence of several pores on the the surface of *Luffa cylindrica* which gives a rough and uneven texture. The presence of pores promotes the dye adsorption.

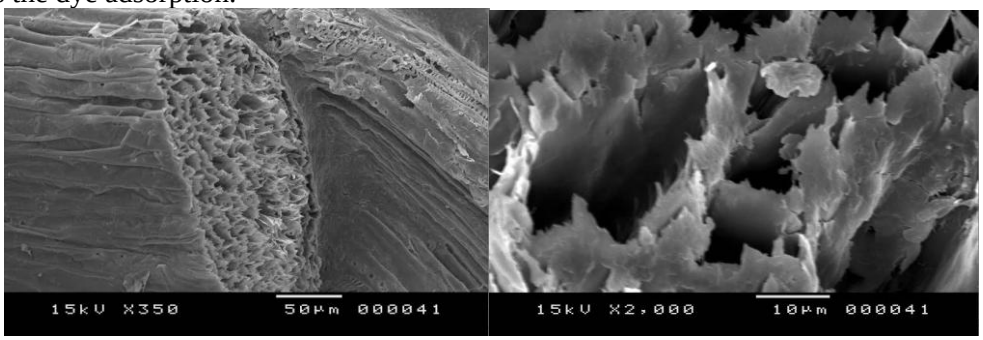

Figure 2. SEM micrographs of *Luffa cylindrica*. (a) 350 ×, (b) 2000×

3.2. Effect of pH

The pH is the most important factor influencing the chemistry of both dye molecule and adsorbent in aqueous solutions. Figure 3 illustrates the biosorption of MB and IC at different pH (2-10) according to reaction time. When initial pH of the MB solution was increased from 2 to 10, biosorption capacity increased from lower to higher. As indicated by others authors, MB biosorption capacities are very important at a higher solution pH [9,20]. This can be explained by the electrostatic attraction between the positively charged MB (solution pH > pKa = 3.8 table 2) and the negatively charged surface of *Luffa cylindrica* (solution pH > pH_{pzc} = 7.85, Table 3). Although, the biosorption capacity of IC increases with decreasing pH in the range of pH 2-10. The possible mechanisms for the effect of pH on biosorption of IC are likely to be ionic interactions [[49]] of the dye anions with the protonated amino groups on the *Luffa cylindrica* (solution pH < pH_{pzc} = 7.85, *Luffa cylindrica* charged positively). This tendency correlated well with the variation of surface charge of *Luffa cylindrica* (the pH_{ZPC} = 7.85). At low pH, surface sites of *Luffa cylindrica* are protonated and have a positively charged. In contrary, at high pH, the surface hydroxides lose their protons and the surface becomes anionic.

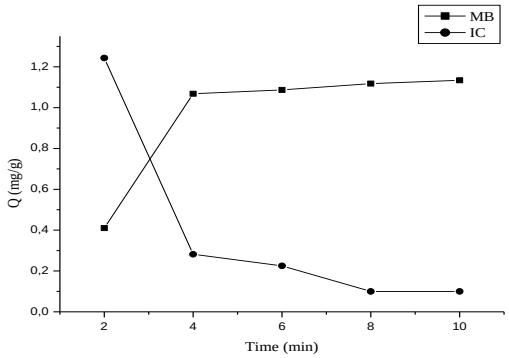

Figure 3. Effect of pH on the biosorption capacity. Temperature: 20 °C, Initial concentration: 20 mg/L, mass of fibers: 0.5 g, volume: 80 ml.

3.3. Effect of contact time and Initial dye concentration

To investigate the ability of *Luffa cylindrica* to eliminate different quantities of MB and IC from aqueous solution and determine times necessary to reach equilibrium, several dye solutions with initial concentrations ranging from 20 to 100 mg/L were studied. According the figures 4 and 5, the biosorption capacity of MB and IC increases a function of contact time at all initial dye concentrations and it remains constant after an equilibrium contact time of about 45 min for MB and 540 min for IC. In addition, the biosorption capacity of MB and IC of time is composed of two parts. In the first part, biosorption capacity increases rapidly for the first 10 min for MB and 150 min for IC but, in the second part; the biosorption is very slow and reaches equilibrium after 45 min for MB and 525 min for IC and for concentration of 100 mg / L with adsorption capacities of 13.33 and 6.44 mg / g, respectively. For both dyes, the higher biosorption capacity during the initial period may be due to the high number of available biosorption site during the earliest stage of the process and no less than 83% for MB and 50% for IC of total dye was removed. However, after this period, the number of sites available for biosorption diminished so that the dye molecules required longer time periods in order to reach the least accessible sites. Similar behaviours were observed in the literature for the dye adsorption by *Posidonia* fibers [17], silk [49] and fiber *Agave america* [16].

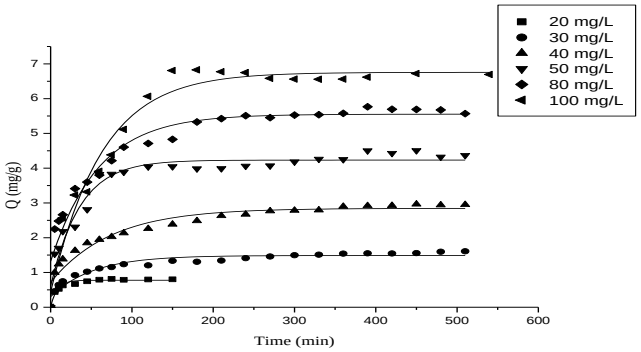

Figure 4. Effect of initial IC concentration on the biosorption capacity. Temperature: 20 °C, pH: 2, mass of fibers: 0.64 g, volume: 80 ml.

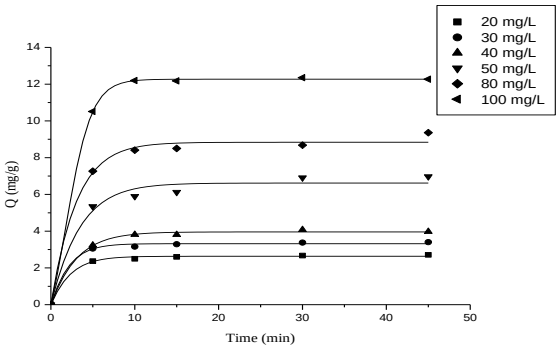

Figure 5. Effect of initial MB concentration on the biosorption capacity. Temperature: 20 °C, pH: 10, mass of fibers: 0.64 g, volume: 80 ml.

3.4. Effect of mass of fibers

The influence of the mass of *Luffa cylindrica* fibers on the elimination of MB and IC was studied. Figure 6 shows the effect of the variation of the mass of fibers on biosorption capacity. It is noted that greater the quantity of fibers in the solution increases, greater the amount of dye retention increases. Indeed, the increase of mass from 0.4 to 1.5 g is followed by an increase of retention rate from 44.09% to 60.24% for IC and from 92.45% to 97.21% for MB. Thereafter it becomes constant. The increase of mass of fibers in the solution is accompanied by an increase number of active sites for retention of dye. Therefore, retention rate of dye increases. These results are similar to those obtained by Kesraoui et al. [14], Rahman et al. [6] and Maghri et al. [9].

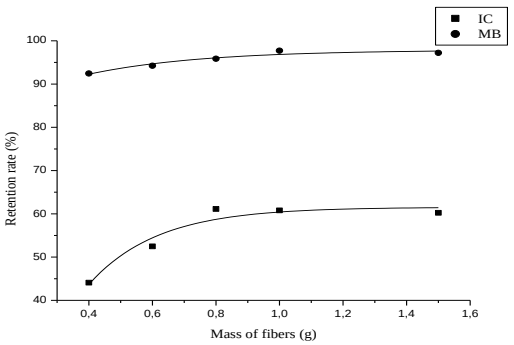

Figure 6. Effect of mass of fibers on the biosorption capacity. pH: (IC :2, MB :10), temperature: 20 °C, Initial concentration: 10 mg/L, volume: 80 ml.

3.5. Effect of salt addition

The study of salt addition is intended on the one hand to simulate the industrial dye baths, on the other hand, to study the influence of ionic strength on adsorption phenomena. In fact, textile industry often added salts to improve the fixation of the dye on the tissue. Figure 7 shows that the adsorbed amount of the IC and MB decreased when adding of NaCl for biosorption. In theory, when the electrostatic forces between the surface of the adsorbent and the adsorbate ions are favorable, an increase in ionic strength decreases the biosorption capacity. Inversely, when the electrostatic forces are repulsive, an elevation in the ionic strength increases the biosorption capacity [15]. The similar results were obtained with our both processes. The addition of 0.5 g NaCl allowed a significant decrease in the amount adsorbed of 16.26 and 32.69% respectively for IC and MB. Sodium ions Na^+ and Cl^- highly mobile appear discharging anionic dyes and decrease their attachment to the surface sites of *Luffa cylindrica* [50].

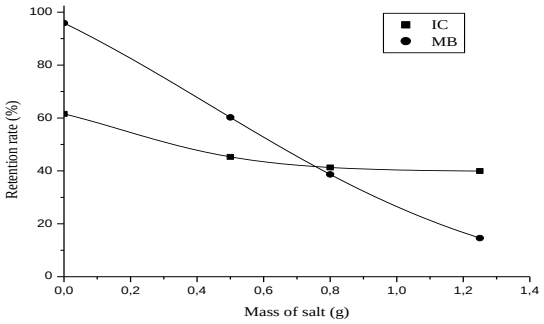

Figure 7. Effect of salt on the biosorption capacity. pH: (IC :2, MB :10), mass of fibers: 0.64 g, temperature: 20 °C, Initial concentration: 10 mg/L, volume: 80 ml.

3.6. Effect of temperature

Temperature is an important parameter for the real application of the biomass. The IC and MB biosorption process was studied at 20, 35, 60 and 70 °C. The investigation of the effect of temperature on the biosorption of dyes by Luffa cylindrica fibers, for initial concentrations of 10, 60, and 85 mg/L, is represented in Figure 8. When the temperatures of dye solution increased from 10 to 70 °C, the biosorption capacities of IC and MB decreased from 5.54 to 4.57 mg/g and 9.46 to 7.56 mg/g for initial concentrations of 85 mg/L and for IC and MB, respectively, with increasing temperature from 10 to 70 °C. This phenomenon may causes an increase in the solubility of the dyes, resulted in a stronger interaction forces between dyes and solvent than those between dyes and *Luffa cylindrica* [51]. This result indicates that the process may be considered as an exothermic process [14]. Similar results were obtained in other studies for the biosorption of methylene blue onto sawdust [16,51].

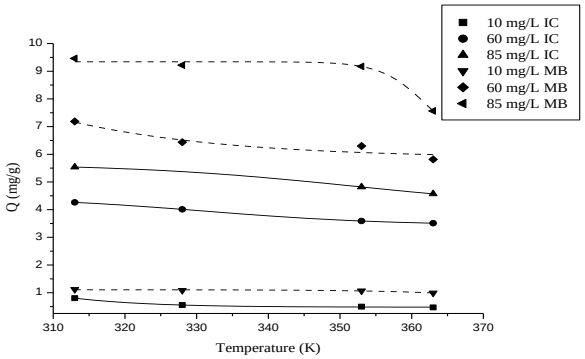

Figure 8. Effect of temperature on the biosorption capacity, Initial concentration: 10 mg/L, pH: 10, mass of fibers: 0.64 g, volume: 75 ml.

3.7. Thermodynamic analysis

In order to qualify the present biosorption of dyes by *Luffa cylindrica*, thermodynamic factors including the Gibbs free energy ΔG° (kJ/mol), enthalpy ΔH° (kJ/mol), and entropy ΔS° (J/mol/K) were calculated for concentrations 10, 60, and 85 mg/L and listed in Table 4. The thermodynamic was studied at 293, 328, 353 and 363 K. The negative value of ΔG° indicates the spontaneous nature of biosorption of IC and MB onto *Luffa cylindrica* [14,51]. ΔG° is varying from -6.004 to -3.066 kJ mol^{-1} and from -0.832 to -0.116 kJ mol^{-1} at 85 mg/L and for MB and IC, respectively. Moreover, these values being within the range -20 to 0 kJ mol^{-1} [52], this process can be considered as physisorption. On the other hand, the positive values of ΔG° for IC biosorption suggest a low affinity of *Luffa cylindrica* fibers for IC at the low dye concentration and at the higher temperature [52]. The negative value of ΔH° confirms the exothermic process [14]. The negative value of ΔS° suggests the probability of favourable adsorption [17].

Table 4. Thermodynamic parameters estimated for IC and MB biosorption by *Luffa cylindrica* at initial concentrations of 10, 60 and 85 mg/L

				ΔG°(kJ.mol^{-1})			
				Temperature (K)			
Dyes	C (mg/L)	ΔH° (kJ .mol^{-1})	ΔS° (J.mol.K^{-1})	293	328	353	363
MB	10	-8.604	-13.751	-4.530	-4.319	-4.586	-3.443
	60	-17.941	-38.926	-6.797	-5.507	-5.127	-4.632
	85	-18.207	-40.730	-6.004	-5.766	-5.983	-3.066
IC	10	-9.752	-32.540	-1.223	1.523	1.966	0.193
	60	-8259,127	-25.839	-0.943	0.102	-0.719	0.451
	85	-5949,498	-17.326	-0.832	-0.719	-1,934	-0.116

3.8. Kinetic data analysis

In order to evaluating the biosorption kinetics of IC and MB into *Luffa cylindrica* fibers, pseudo first-order, pseudo second-order, Elovich and Brouers-Sotolongo equations were investigated to test the experimental data. The analyses were carried out using the nonlinear regression analysis using orgin"6.0". In fact, the study of kinetic results of the models analysed by nonlinear approaches present a great interest to investigate the best model that describes the biosorption process. The modeling results such as: the rate constants, the experimental and calculated equilibrium biosorption capacities, the linear regression coefficients and nonlinear chi-square test obtained at all concentrations were represented in Tables 5 and 6. The best-fit model was chosen according to a linear regression correlation coefficient (R^2), the calculated Qe values and nonlinear chi-square test (χ^2). The correlation coefficients obtained by the pseudo-first-order and Elovich model at all initial IC and MB concentrations were found to be less than 0.966 and 0.993 respectively while, the nonlinear chi-square test are high than 0.002 and 0.003 for IC and MB, respectively. However, in the same, the theoretical Qe_1 did not give acceptable values. Both pseudo-second order and Brouers-Sotolongo kinetic models presented a good fitting for biosorption process. However, Brouers-Sotolongo kinetic model had higher correlation coefficients ($R^2 > 0.965$ for IC and 0.992 for MB) and the lower nonlinear chi-square test ($\chi^2 <$ 0.147 for IC and 0.128 for MB). Whereas the second-order model shows satisfactory fit with the experimental data related to the biosorption of IC onto *Luffa cylindrica* with high R^2 (0.993). Moreover, as shown in Tables 5 and 6, the calculate Qe^2 are quite similar to the experimental values for IC, but, the Qe calculated by Brouers Sotolongo model did not give acceptable values for IC.

Table 5. Constants of biosorption kinetics of IC into *Luffa Cylindrica* fibers

	Initial IC concentration (mg/L)					
Kinetic models	20	30	40	50	80	100
$Qe_{,exp}$ ($mg.g^{-1}$)	0.083	1.610	2.950	4.370	5.568	6.696
Pseudo-first-order						
Calculated Qe_1($mg.g^{1}$)	0.775	1.444	2.716	4.192	5.378	6.734
k_1(min^{-1})	0.125	0.033	0.028	0.036	0.031	0.017
R^2	0.966	0.893	0.858	0.9325	0.873	0.952
χ^2	0.002	0.019	0.088	0.099	0.295	0.192
h_1	0.096	0.047	0.076	0.151	0.166	0.114
Pseudo-second-order						
Calculated Qe_2($mg.g^{-1}$)	0.836	1.566	2.939	4.491	5.767	7.598
k_2 ($mg.g^{-1}.min^{-1}$)	0.230	0.032	0.015	0.013	0.009	0.003
R^2	0.991	0.993	0.991	0.964	0.973	0.962
χ^2	0.006	0.0008	0.007	0.053	0.037	0.151
h_2($mg.g^{-1}.min^{-1}$)	0.160	0.078	0.129	0.262	0.299	0.173
Elovich						
A	0.113	0.244	0.455	0.660	0.852	1.369
A	113.4	5.821	3.033	3.253	2.328	0.309
R^2	0.935	0.965	0.944	0.915	0.949	0.862
χ^2	0.012	0.006	0.035	0.0761	0.118	0.323
Brouers–Sotolongo n = 2						
Calculated Qe ($mg.g^{-1}$)	0.879	2.107	5.395	4.760	7.759	7.428
τ	5.290	53.049	267.564	18.743	48.475	40.589
A	0.790	0.497	0.374	0.777	0.477	1.088
R^2	**0.993**	**0.995**	**0.998**	**0.997**	**0.988**	**0.965**
χ^2	0.005	0.0007	0.001	0.014	0.028	0.147

The highest R^2 values are in bold and the lowest χ^2 underlined.

These results demonstrate that the pseudo-second-order model is able to describe satisfactorily the kinetic behavior of MB biosorption by *Luffa cylindrica* fibers. While for MB, both pseudo-second order and Brouers-Sotolongo kinetic models showed that calculated Qe is closer to the experimental Qe. In addition, the initial adsorption rate (h_1 and h_2) and the rate constant (k_1 and k_2) were found to increase for MB. This result indicates that the rates of MB biosorption onto *Luffa cylindrica* are much faster than IC. On the other hand, the Brouers-Sotolongo kinetic model determines the time necessary to biosorb half the maximum quantity ($\tau_{50\%}$), and then can measure the speed of the reaction. Brouers [33] showed that for n = 2, $\tau_c = \tau_{50\%}$. As shown Tables 5 and 6, 5 - 40 min for IC and 0.5 – 2 min for MB are sufficient to reach half of the uptake capacities. Such values are very importantes mainly for industrial.

Table 6. Constants of biosorption kinetics of MB into *Luffa Cylindrica* fibers

Kinetic models	Initial MB concentration (mg/L)					
	20	30	40	50	80	100
$Qe_{,exp}$ ($mg.g^{-1}$)	2.765	3.454	4.040	7.035	9.395	13.337
Pseudo-first-order						
Calculated Qe_1($mg.g^{-1}$)	2.700	3.407	4.001	6.909	9.217	12.905
k_1(min^{-1})	0.390	0.427	0.320	0.250	0.287	0.324
R^2	0.993	0.993	0.996	0.981	0.987	0.984
χ^2	0.004	0.007	0.005	0.084	0.098	0.239
h_1	1.053	1.454	1.280	1.727	2.645	4.181
Pseudo-second-order						
Calculated Qe_2($mg.g^{-1}$)	2.275	3.473	4.101	7.160	9.514	13.270
k_2 ($mg.g^{-1}.min^{-1}$)	0.408	0.376	0.211	0.074	0.068	0.059
R^2	0.9990	0.9990	0.997	0.996	0.9971	0.991
χ^2	0.0003	0.001	0.004	0.041	0.022	0.130
h_2($mg.g^{-1}.min^{-1}$)	2.111	4.535	3.548	3.793	6.155	10.389
Elovich						
A	0.106	0.113	0.169	0.470	0.542	0.687
A	$5.431*10^{10}$	$1.625*10^{12}$	$1.435*10^{9}$	69601	$6.222*10^{5}$	$3.078*10^{6}$
R^2	0.893	0.880	0.657	0.847	0.840	0.825
χ^2	0.001	0.0026	0.023	0.060	0.084	0.151
Brouers–Sotolongo n = 2						
Calculated Qe ($mg.g^{-1}$)	2.790	3.529	4.036	7.240	9.575	13.889
τ	0.532	0.334	2.249	1.616	1.363	0.509
A	0.760	0.674	1.756	0.863	0.902	0.549
R^2	**0.9997**	**0.9994**	**0.9987**	**0.997**	**0.9972**	**0.9924**
χ^2	0.0002	0.0007	0.0021	0.014	0.024	0.128

The highest R^2 values are in bold and the lowest χ^2 underlined

3.9. Adsorption isotherm modeling

It is essential to determine the most suitable correlation for the equilibrium curves, in order to optimize biosorption process to eliminate dyes. The isotherms data were analyzed using eight equilibrium models: Freundlich, Langmuir, Temkin, Jovanovic, Brouers-Sotolongo, Redlich–Peterson, Sips and Toth isotherm models. The graphic correlation between the experimental data and the theoretical models for the biosorption systems are given in Figures 7 and 8 for MB and IC, respectively. Tables 7 and 8 show the values of the maximum biosorption capacity (Q_m), correlation coefficient (R^2) values, nonlinear chi-square test (χ^2), and the other parameters for all the isotherms studied.

Redlich–Peterson model is a hybrid isotherm between Langmuir and Freundlich models (Vergas et al. 2011). The equilibrium biosorption data were very well represented by Freundlich isotherms with high correlation coefficients of 0.999 for IC and low nonlinear chi-square test (χ^2 = 0.021). But for MB, this isotherm is not satisfactorily fit with the biosorption process (R^2 = 0.950). The Toth isotherm is another empirical equation to improve the fit of the Langmuir isotherm (Foo et al. 2010). It describes heterogeneous adsorption process. Among all the isotherms investigated for IC, the value of Q_m equal to 6.876 mg/g found in the fit of the Toth isotherm was the value closest to the experimental one

of 6.874 mg/g. This shows that the isotherm can be satisfactorily used in the biosorption of IC. Like Redlich–Peterson, Toth isotherm represents for IC high correlation coefficients of 0.996 for and low nonlinear chi-square test (χ^2 = 0.036) but for MB, Toth isotherm is less adequate to explain the biosorption process (R^2 = 0.969 and χ^2 = 0.999).

Sips isotherm is a mixed form of Langmuir and Freundlich isotherm models. This model predicts the heterogeneous adsorption systems [42]. At low dye concentrations, the Sips equation is reduced to the Freundlich equation [39]. Table 7 shows that the value of nonlinear chi-square test for MB (χ^2 = 0.329) is low. On the other hand, the Q_m value of 14.193 mg/g for MB obtained for this isotherm is close to the experimental value of Q_m (13.900 mg/g), the value of R^2 of 0.990 shows good fitting of this isotherm to the experimental data (Table 7 and 8). For the case of IC, Sips isotherm is less adequate to explain the biosorption process (R^2 = 0.978). The experimental data were best described by the Brouers-Sotolongo for MB. Indeed, the Brouers-Sotolongo model provides the best fit by giving the highest non-linear R^2 (0.992) and the lowest nonlinear chi-square test (χ^2 = 0.256). In addition, table 7 shows a Q_m value (13.849 mg/g) is close to the $Q_{m,exp}$ value equal to 13.900 mg/g. As Sips, Brouers-Sotolongo isotherm for IC is less adequate to explain the biosorption process (R^2 = 0.989 and χ^2 = 0.112). Langmuir's isotherm is known as monolayer adsorption onto a homogeneous surface with a finite number of active sites and with equal energy [53]. The fit to experimental data (R^2 = 0.885 for MB and 0.959 for IC) in Figures 7 and 8 shows that the Langmuir isotherm is less adequate to explain the biosorption of dyes onto *Luffa Cylindrica*, as compared to the Brouers-Sotolongo, Sips and Toth isotherms. Like the Langmuir isotherm, the Jovanovic isotherm considers a monolayer and no lateral interactions. The values R^2 (0.915 and 0.976 for MB and IC, respectively) show that Jovanovic isotherm is not suitable to fit the isotherm curves for biosorption of dyes onto *Luffa cylindrica*. The Freundlich isotherm is an empirical equation used for heterogeneous systems with interaction between the molecules adsorbed [49]. The n values ranging between 1 and 10 is a measure of adsorption intensity or surface heterogeneity, becoming more heterogeneous as its value gets closer to 10 [14]. Furthermore, the value of Freundlich exponent n was equal to 2.004 for MB and 2.143 for IC, both were in the 1–10 range indicating favourable adsorption [32]. Tables 7 and 8 show the correlation coefficient and Figures 7 and 8 clearly show that the former model fitted the equilibrium data is the lowest (R^2 = 0.786 for MB and 0.893 for IC), thus confirming the poor applicability of Freundlich isotherm for this type of sorption process. Like the Freundlich isotherm, the Temkin isotherm regards the interactions between adsorbates assuming that the bisorption heat of all molecules decreases linearly when the layer is covered and that the biosorption has a maximum energy distribution of uniform bond. The constant b_T is related to the heat of adsorption and the positive value found (b_T = 521.276 for MB and 1170.149 for IC) indicates an exothermic process. The Temkin isotherm shows a low correlation coefficient (R^2 = 0.913 for MB and 0.934 for IC), just like Langmuir, Freundlich and Janovic isotherm.

Comparison of dyes biosorption by *Luffa cylindrica* fibers and other low-cost adsorbents to establish the relative efficiency of *Luffa cylindrica* for biosorption of MB and IC relative to others used low-cost adsorbents; a comparison was made on the basis of the biosorption capacity (Q_m). To determine the efficacity of *Luffa cylindrica* to remove MB and IC, a comparison with other low-cost adsorbents was realized according to the biosorption capacity (Qm). According to the comparative study, the results (Table 7) have shown that the Luffa cylindrica fibers may be considered as a promising biomaterial to eliminate MB when compared to *Posidonia oceanica* [32], *Agave americana* [16], Algae Carolina [54] and Langsat peel [20]. Several studies have the values of Q_m for the biosorption of IC lower than the *Luffa cylindrica* such as: Mytilus Edulis shell [9], Fly ash [55], Hen Feathers [8] and mixing zeolite [56].

Despite its low biosorption capacity, the *Luffa cylindrica* had a better potential of biosorption compared to other cheap natural materials.

Table 7. Freundlich, Langmuir, Temkin, Jovanovic, Brouers-Sotolongo, Redlich–Peterson, Sips and Toth model constants and correlation coefficients for the biosorption of MB onto *Luffa cylindrica* fibers. ($Q_{m,exp}$ = 13.900 mg/g)

Freundlich	Langmuir	Temkin	Jovanovic
Two parameters isotherm modals			
R^2 = 0.786	R^2 = 0.886	R^2 = 0.786	R^2 = 0.915
k_F = 3.155	k_L= 0.145	b_r = 521.275	K_j = - 0.172
n = 2.004	Q_m = 19.319	A_T = 1.147	Q_m = 14.849
χ^2 = 6.262	χ^2 = 3.346	χ^2 = 2.550	χ^2 =2.486
Brouers-Sotolongo	Redlich–Peterson	Sips	Toth
Three parameters isotherm models			
R^2 = 0.992	R^2 = 0.951	R^2 = 0.990	R^2 = 0.969
K_{av} = 0.070	K_{rp} = 0.004	K_s = 2.500	$K_T = 2.686\times10^{10}$
Q_m = 13.849	Q_m = 15.348	Q_m =14.193	Q_m = 13.861
α = 1.908	n = 2.016	m_s = 19.000	n = 12.147
χ^2 = 0.256	χ^2 = 1.624	χ^2 = 0.329	χ^2 = 2.550

Table 8. Freundlich, Langmuir, Tempkin, Jovanovic, Brouers-Sotolongo, Redlich–Peterson, Sips and Toth model constants and correlation coefficients for the biosorption of IC onto *Luffa Cylindrica* fibers. ($Q_{m,exp}$ = 6.874 mg/g)

Freundlich	Langmuir	Temkin	Jovanovic
Two parameters isotherm modals			
R^2 = 0.983	R^2 = 0.959	R^2 = 0.934	R^2 = 0.976
k_F = 0.906	k_L= 0.030	b_r = 1170.149	K_j = - 0.037
n = 2.143	Q_m = 9.554	A_T = 0.328	Q_m = 7.357
χ^2 = 0.885	χ^2 = 0.336	χ^2 = 0.457	χ^2 = 0.195
Brouers-Sotolongo	Redlich–Peterson	Sips	Toth
Three parameters isotherm models			
R^2 = 0.989	R^2 = 0.999	R^2 = 0.978	R^2 = 0.996
K_{av} = 0.014	$K_{rp} = 1.000\times10^{-6}$	K_s = 1.597	$K_T = 3.966\times10^{11}$
Q_m = 7.021	Q_m = 7.633	Q_m = 7.681	Q_m = 6.876
α = 1.332	n = 2.543	m_s = 116.468	n = 7.265
χ^2 = 0.112	χ^2 = 0.021	χ^2 = 0.212	χ^2 = 0.036

Table 9. Comparison of biosorption isotherm characteristics between *Luffa cylindrica* fibres and other studied sorbents for MB and IC.

Sorbents	MB Q_m (mg/g)	References	Sorbents	IC Q_m (mg/g)	References
Luffa cylindrica	13.9	This study	*Luffa Cylindrica*	6.874	This study
Posidonia oceanic	5.518	[32]	Silk	15.06	[49]
Mytilus Edulis shell	17.12	[9]	Mytilus Edulis shell	2.11	[9]
Agave americana	6	[16]	Charcoal	9.275	[7]
Algae Carolina	6	[54]	Fly ash	1.48	[55]
Langsat peel	8	[20]	mixing zeolite	0.583	[56]
Macroalgae	75	[19]	Hen Feathers	3.205	[8]

4. Conclusion

Starting from the results described above, it can be concluded that *Luffa cylindrica* fibers are composed of 54.00 % of cellulose, 23.00 % of hemicellulose, 4.70 % of pectin, 11.20% of lignin and 7.10 % of fats and waxes. While, the roots are composed by 20.37% of cellulose, 29.04% of hemicellulose, 31.39% of pectin, 9.95% of lignin and 9.25 of fats and waxes. The present study shows that the *Luffa ylindrica* fibers were applied successfully for the biosorption of MB and IC. The best IC and MB biosorption was found at pH 2 and 10, respectively. In addition, the increase in the temperature of solution decreases the biosorbed quantity. While for higher values of the mass of biomass, the retention rate of dyes by the *Luffa cylindrica* increases. The addition of NaCl decreased greatly the amount biosorbed because of the reduction of the electrostatic forces between the adsorbate and the adsorbent. The analysis of all the isotherms models were evaluated using the important parameter (Q_m, R^2 and χ^2), the isotherms can be orderly according to their capacity to predict the experimental behaviour between dyes and adsorbant. With respect to R^2 and χ^2 for MB (in descending order): Brouers–Sotolongo > Sips > Toth>Redlich– Peterson> Jovanovic, >Temkin > Langmuir> Freudlich and for IC: Redlich– Peterson > Toth > Brouers–Sotolongo > Sips > Janovic > Temkin > Langmuir > Freudlich. With respect to Q_m for MB (in descending order): Brouers–Sotolongo >Toth> Sips > Jovanovic >Redlich– Peterson > Langmuir and for IC: Toth > Brouers–Sotolongo > Janovic > Redlich– Peterson > Sips > Langmuir. Equilibrium data were best described by Brouers-Sotonlongo for MB with maximum biosorption capacity of 13.849 mg/L. While for IC, the Toth isotherm model is the best model describing the mechanism of biosorption with maximum biosorption capacity of 6.876 mg/L. The thermodynamic study showed that the biosorption of IC and MB is an exothermic process and spontaneous while the kinetic study showed that the process follows the fractal kinetic model of Brouers-Sotolongo (2,α) model.

Acknowledgement-The authors express their sincere gratitude to the FP7 FP4BATIW Euro-Mediterranean project and Laboratory of Energy and Materials for the financial support of this study.

References

[1] K. Sumanjit, S. Rani, R. Kumar Mahajan, *Journal of Chemistry*., 2013 (2013) 1-12.
[2] E.R. García, R.L. Medina, M.M. Lozano, I.H. Pérez, M.J. Valero, A.M. Maubert Franco, *Materials.*, 7 (2014) 8037-8057.
[3] O.S. Bello, I.A. Bello, K.A. Adegoke, *A Review. S. Afr. J. Chem.*, 66 (2013) 117-129.
[4] M. Khodaie, N. Ghasemi, B. Moradi, M. Rahimi, *Journal of Chemistry*., 2013 (2013) 1-6.
[5] S. Álvarez-Torrellas, R. García-Lovera, A. Rodríguez, J. García, *Chemical Engineering Transactions.*, 43 (2015) 1963-1968.
[6] M.A. Rahman, S.M.R Amin, A.M. Shafiqul Alam, *Dhaka Univ. J. Sci*., 60(2) (2012)185-189.
[7] R. Jain, M. Mathur, S. Sikarwar, *Journal of Scientific & Industrial Research*., 65 (2006) 258-263.
[8] A. Mittal, J. Mittal, L. Kurup, Batch and bulk removal of hazardous dye, indigo Carmine from wastewater through adsorption», Department of Applied Chemistry, National Institute of Technology, India, (2006).
[9] I. Maghri, A. Kenz, M. Elkouali, O. Tanane, M. Talbi, *J. Mater. Environ. Sci*., 3 (1) (2012) 121-136.
[10] K. Majewska-Nowak, J. Kawiecka-Skowron, *Desalination and Water Treatment*., 34 (2011) 367-373.
[11] S. Caprarescu, A.R. Miron, V. Purcar, A.L. Radu, A. Sarbu, D. Ion-Ebrasu, L.I. Atanase, M. Ghiurea, *Water Science et Technology.*, In press (2016).
[12] M.L. Meshram, D.H. Lataye, *International Journal of Engineering Research & Technology*., 3(11) (2014) 1216-1220.

[13] V. Karthik, K. Saravanan, P. Bharathi, V. Dharanya, C. Meiaraj, *J Chem Pharm Sci*., 7 (2014) 301-307.
[14] A. Kesraoui, A. Moussa, G. Ben Ali, M. Seffen, *Environ Sci Pollut Res*., 2015 (2015) 1-9.
[15] A. Kesraoui, T. Selmi, M. Seffen, F. Brouers, *Environ Sci Pollut Res*., In press (2016).
[16] A.M. Ben Hamissa, F. Brouers, M.C. Ncibi, M. Seffen, *Sep Sci Technol.*, 48 (2013) 1-9.
[17] M.C. Ncibi, B. Mahjoub, M. Seffen, *Int J Environ Sci Technol*., 4(4) (2007) 433-440.
[18] S.M. Kanawade, R.W. Gaikwad, *International Journal of Chemical Engineering and Applications*., 2 (5) (2011) 317-319.
[19] E. Daneshvar, A. Vazirzadeh, A. Niazi, M. Sillanpää, A. Bhatnagar, *Chemical Engineering Journal*., 307 (2016) 435-446.
[20] M.A.M. Salleh, D. Khalid Mahmoud, N.A. Binti Awang Abu, W.A.W. Abdul Karim, A.B. Idris, *Journal of Purity, Utility Reaction and Environment*., 1(10) (2012) 472-495.
[21] A. Nasrullah, H. Khan, A. Sada Khan, Z. Man, N. Muhammad, M.I. Khan, N.M. Abd El-Salam, *The Scientific World Journal*., (2015).
[22] A.N. Osuagwu, H.O. Edeoga, *Journal of Agriculture and Veterinary Science*., 7 (2014) 41-44.
[23] I.O. Mazali, O.L. Alves, *An Acad Bras Cienc*., 77(1) (2005) 25-31.
[24] D.B. Adie, S.B. Igboro, N. Daouda, *Am.Int.J Contemp.Res.*, 3(3) (2013) 117-123.
[25] H. Demir, A. Top, D. Balkose, S. Ulk, *J Hazard Mater.*, 153 (2008) 389-394.
[26] T. Sedan, Etude des interactions physico-chimiques aux interfaces fibres de chanvre/ciment. Influence sur les propriétés mécaniques du composite. Thesis, Limoges University, (2007).
[27] K.H. Mahmoudi, N. Hamdi, E. Srasra, *Korean J. Chem. Eng.*, 32(2) (2015) 274-283.
[28] S.K. Milongic, V. Antonucci, M. Minutoli, N. Giordano, *Carbon*., 27 (1975) 337-347.
[29] Ho Y.S., McKay G. *Chemical Engineering Journal*. 70 (2) (1998) 115-124.
[30] S. Thirumalisamy, M. Subbian, *Bioressorces*., 5(1) (2010) 419-437.
[31] F. Brouers, O. Sotolongo-Costa *Physica A.*, 368 (2006) 165-175.
[32] M.C. Ncibi, B. Mahjoub, M. Seffen, *Adsorpt Sci Technol*., 24 (2006) 461-473.
[33] Brouers F. *Journal of Modern Physics.* 5 (2014) 1594-1601.
[34] F. Brouers, T.J. Al-Musawi, *J.of Molecular Liquids.*, 212 (2015a) 46-51.
[35] I.W., Burr, *The Annals of Mathematical Statistics*, 13 (1942) 215-232.
[36] F. Brouers, *Open Journal of Statistics.*, 5 (2015b) 730-741.
[37] I. Langmuir, *J. Am. Chem Soc.*, 38 (1916) 2221-2295.
[38] H. Freundlich, *Z. Phys. Chem*., 57 (1906) 385-470.
[39] A.M.M. Vargas, A.L. Cazetta, M.H. Kunita, T.L. Silva, V.C. Almeida, *Chem Eng J.*, 168 (2011) 722-730.
[40] M.I. Temkin, *J.Phys.Chem*., 15 (1941) 233-296.
[41] P.S. Kumar, S. Ramalingam, M. Niranjanaa, P. Vijayalakshmi, S. Sivanesan, *Desalination*., 261 (1) (2010) 52-60.
[42] K.Y. Foo, B.H. Hameed, *Chemical Engineering Journal.*, 156 (2010) 2-10.
[43] L. Jiménez, A. Pérez, M.J. De La Torre, A. Moral, L. Serrano, *Bioresource Technology*., 98(18) (2008) 3487-3490.
[44] I. Miranda, J. Gominho, H. Pereira, *BioResources*., 7(3) (2012) 4350-4361.
[45] R. Khiari, E. Mauret, M.N. Belgacem, F. Mhenni, *BioResources*., 6(1) (2011) 265-281.
[46] S. Mansouri, R. Khiari, N. Bendouissa, S. Saadallah, E. Mauret, F. Mhenni, *Ind Crops Prod*., 36 (2012) 22-27.
[47] N. Ben Douissa, S. Dridi-Dhaouadi, F. Mhenni, *Journal of Water Process Engineering.*, 2 (2014) 1-9.

[48] M.A. Ahmad, N.A.A. Puad, O.S. Bello, *Water Resources and Industry.*, 6 (2014) 18-35.
[49] N. Jiwalak, S. Rattanaphani, J.B. Bremner, V. Rattanaphani, *Fibers and Polymers.*, 11(4) (2010) 572-579.
[50] F. Krika, N. Azzouz, M.C. Ncibi, *Int. J. Environ. Res.*, 6(3) (2012) 719-732.
[51] A.M. Aljeboree, A.N. Alshirifi, A.F. Alkaim, *Arabian Journal of Chemistry*, (2014).
[52] A.M. Ben Hamissa, A. Lodi, M. Seffen, E. Finocchio, R. Botter, A. Converti, *Chemical Engineering Journal*., 159 (2010) 67-74.
[53] V. Patrulea, A. Negrulescu, M.M. Mincea, L.D. Pitulice, O.B. Spiridon, V. Ostafe, *BioResources*., 8 (2013) 1147-1165.
[54] H.H. Hammud, L.M.A. Fayoumi, H. Holail, E.S.M.E. Mostafa, *Int.J.Chem.*, 3(4) (2011) 147-163.
[55] E.M. De Carvalho, D.A. Fungaro, C.P. Magdalena, P. Cunico, *J Radioanal Nucl Chem*., 289 (2011) 617-626.
[56] A. Fungaro, M. Yamaura, T.E.M. Carvalho, *J. At. Mol. Sci.*, 2(4) (2011) 305-316.